

This discussion paper is/has been under review for the journal Atmospheric Chemistry and Physics (ACP). Please refer to the corresponding final paper in ACP if available.

# Air quality and radiative forcing impacts of anthropogenic volatile organic compound emissions from ten world regions

M. M. Fry<sup>1</sup>, M. D. Schwarzkopf<sup>2</sup>, Z. Adelman<sup>1</sup>, and J. J. West<sup>1</sup>

<sup>1</sup>Department of Environmental Sciences and Engineering, University of North Carolina at Chapel Hill, Chapel Hill, North Carolina, USA

<sup>2</sup>NOAA Geophysical Fluid Dynamics Laboratory, Princeton, New Jersey, USA

Received: 21 May 2013 – Accepted: 31 July 2013 – Published: 13 August 2013

Correspondence to: J. J. West (jjwest@email.unc.edu)

Published by Copernicus Publications on behalf of the European Geosciences Union.

ACPD

13, 21125–21157, 2013

Air quality and RF  
impacts of VOC  
emissions

M. M. Fry et al.

<a href="#">Title Page</a>	
<a href="#">Abstract</a>	<a href="#">Introduction</a>
<a href="#">Conclusions</a>	<a href="#">References</a>
<a href="#">Tables</a>	<a href="#">Figures</a>
<a href="#">◀</a>	<a href="#">▶</a>
<a href="#">◀</a>	<a href="#">▶</a>
<a href="#">Back</a>	<a href="#">Close</a>
<a href="#">Full Screen / Esc</a>	
<a href="#">Printer-friendly Version</a>	
<a href="#">Interactive Discussion</a>	



## Abstract

Non-methane volatile organic compounds (NMVOCs) influence air quality and global climate change through their effects on secondary air pollutants and climate forcers. Here we simulate the air quality and radiative forcing (RF) impacts of changes in ozone, 5 methane, and sulfate from halving anthropogenic NMVOC emissions globally and from 10 regions individually, using a global chemical transport model and a standalone radiative transfer model. Halving global NMVOC emissions decreases global annual average tropospheric methane and ozone by 36.6 ppbv and 3.3 Tg, respectively, and surface ozone by 0.67 ppbv. All regional reductions slow the production of PAN, resulting 10 in regional to intercontinental PAN decreases and regional NO<sub>x</sub> increases. These NO<sub>x</sub> increases drive tropospheric ozone increases nearby or downwind of source regions in the Southern Hemisphere (South America, Southeast Asia, Africa, and Australia). Some regions' NMVOC emissions contribute importantly to air pollution in other 15 regions, such as East Asia, Middle East, and Europe, whose impact on US surface ozone is 43 %, 34 %, and 34 % of North America's impact. Global and regional NMVOC reductions produce widespread negative net RFs (cooling) across both hemispheres from tropospheric ozone and methane decreases, and regional warming and cooling from 20 changes in tropospheric ozone and sulfate (via several oxidation pathways). The total global net RF for NMVOCs is estimated as 0.0277 W m<sup>-2</sup> (~ 1.8 % of CO<sub>2</sub> RF since the preindustrial). The 100 yr and 20 yr global warming potentials (GWP<sub>100</sub>, GWP<sub>20</sub>) are 2.36 and 5.83 for the global reduction, and 0.079 to 6.05 and -1.13 to 18.9 among the 10 regions. The NMVOC RF and GWP estimates are generally lower than previously modeled estimates, due to differences among models in ozone, methane, and sulfate sensitivities, and the climate forcings included in each estimate. Accounting for 25 a fuller set of RF contributions may change the relative magnitude of each region's impacts. The large variability in the RF and GWP of NMVOCs among regions suggest that regionally-specific metrics may be necessary to include NMVOCs in multi-gas climate trading schemes.

## Air quality and RF impacts of VOC emissions

M. M. Fry et al.

[Title Page](#)

[Abstract](#)

[Introduction](#)

[Conclusions](#)

[References](#)

[Tables](#)

[Figures](#)

[◀](#)

[▶](#)

[◀](#)

[▶](#)

[Back](#)

[Close](#)

[Full Screen / Esc](#)

[Printer-friendly Version](#)

[Interactive Discussion](#)



# 1 Introduction

Non-methane volatile organic compounds (NMVOCs) are chemically reactive gases emitted worldwide from natural and anthropogenic sources. NMVOCs impact air quality and climate by contributing to tropospheric photochemistry (e.g., ozone ( $O_3$ ) production) and aerosol formation. Because of their influence on short-lived climate forcers (e.g.,  $O_3$ , methane ( $CH_4$ ), aerosols), NMVOC reductions could help slow the near-term rate of climate change (Shindell et al., 2012). Here we evaluate the net climate and air quality effects of anthropogenic NMVOC emission reductions, to inform future policies that may address air quality and climate change.

Tropospheric  $CH_4$  and  $O_3$  are the largest greenhouse gas contributors to global anthropogenic radiative climate forcing (RF) behind carbon dioxide ( $CO_2$ ) with abundance-based RFs of  $0.48 \pm 0.05 \text{ W m}^{-2}$  and  $0.35 (-0.1, +0.3) \text{ W m}^{-2}$ , respectively (Forster et al., 2007). Tropospheric sulfate ( $SO_4^{2-}$ ) has produced a global net RF of  $-0.40 \pm 0.2 \text{ W m}^{-2}$  (direct effect only) (Forster et al., 2007). NMVOCs and carbon monoxide (CO) emissions together have contributed an estimated global mean RF of  $0.21 \pm 0.10 \text{ W m}^{-2}$  due to  $O_3$  and  $CH_4$  (1750 to 1998) (Shindell et al., 2005; Forster et al., 2007) and  $0.25 \pm 0.04 \text{ W m}^{-2}$  (1750 to 2000) when  $SO_4^{2-}$ , nitrate ( $NO_3^-$ ), and  $CO_2$  impacts are included (Shindell et al., 2009). More recently, the anthropogenic RF of NMVOC emissions (for 1850–2000) was estimated as  $0.090 \text{ W m}^{-2}$  (due to changes in  $O_3$ ,  $CH_4$ , and  $CO_2$ ) as part of the Atmospheric Chemistry and Climate Model Intercomparison Project (ACCMIP) (Stevenson et al., 2013).

NMVOCs are mainly oxidized by the hydroxyl radical ( $OH$ ) in the troposphere, producing peroxy radicals ( $RO_2$ ) and hydroperoxy radicals ( $HO_2$ ) that then oxidize nitric oxide ( $NO$ ) to yield  $O_3$ . Because thousands of NMVOC species with varying lifetimes (from fractions of a day to months) and chemical reactivities have been documented, global chemical transport models (CTMs) use simplified representations of NMVOCs and reaction pathways (Ehhalt et al., 2001; Prather et al., 2001; Ito et al., 2007). Under high nitrogen oxide ( $NO_x = NO + NO_2$ ) concentrations, NMVOCs contribute to the

## Air quality and RF impacts of VOC emissions

M. M. Fry et al.

[Title Page](#)

[Abstract](#)

[Introduction](#)

[Conclusions](#)

[References](#)

[Tables](#)

[Figures](#)

◀

▶

◀

▶

[Back](#)

[Close](#)

[Full Screen / Esc](#)

[Printer-friendly Version](#)

[Interactive Discussion](#)



## Air quality and RF impacts of VOC emissions

M. M. Fry et al.

Title Page

Abstract

Introduction

Conclusions

References

Tables

Figures

◀

▶

◀

▶

Back

Close

Full Screen / Esc

Printer-friendly Version

Interactive Discussion



efficient cycling between OH and HO<sub>2</sub> and hence, O<sub>3</sub> production, while under low-NO<sub>x</sub> conditions OH depletes, resulting in NMVOC and CH<sub>4</sub> accumulation (Collins et al., 2002). CH<sub>4</sub> is a longer-lived O<sub>3</sub> precursor (perturbation lifetime of ~ 12 yr) (Forster et al., 2007) that decreases as tropospheric OH increases (from NMVOC reductions), resulting in long-term O<sub>3</sub> decreases, in addition to direct, short-term O<sub>3</sub> decreases (Prather et al., 1996; Wild et al., 2001; Fiore et al., 2002; Naik et al., 2005). NMVOC emissions also affect O<sub>3</sub> at local to intercontinental scales, given that the lifetimes of tropospheric O<sub>3</sub> (~ 22 days) (Stevenson et al., 2006) and some NMVOCs (e.g., ethane, benzene) can exceed typical intercontinental transport times (5 to 10 days) (Fiore et al., 2009; West et al., 2009a). NMVOC reductions indirectly influence sulfate aerosol (SO<sub>4</sub><sup>2-</sup>) formation via gas-phase oxidation of sulfur dioxide (SO<sub>2</sub>) by OH, and aqueous-phase oxidation of SO<sub>2</sub> by H<sub>2</sub>O<sub>2</sub> or O<sub>3</sub> (Unger et al., 2006; Leibensperger et al., 2011). NMVOCs are also precursors to secondary organic aerosols (SOA), and influence NO<sub>3</sub><sup>-</sup> aerosol abundance via oxidant changes (Ehhalt et al., 2001; Bauer et al., 2007; Hoyle et al., 2009).

Previous studies have shown that the RF and global warming potential (GWP) of NMVOCs, like other short-lived O<sub>3</sub> precursors, depend on emissions location given their short lifetime in the troposphere (Naik et al., 2005; Berntsen et al., 2006; Forster et al., 2007; and Fry et al., 2012), but few studies quantify the range among different source regions. Fry et al. (2012) calculated 100 yr and 20 yr GWPs (GWP<sub>100</sub>, GWP<sub>20</sub>) of  $4.8 \pm 2.4$  to  $8.3 \pm 1.9$  and  $15.5 \pm 6.8$  to  $26.5 \pm 5.3$ , respectively, for anthropogenic NMVOCs from four regions (due to O<sub>3</sub>, CH<sub>4</sub>, and SO<sub>4</sub><sup>2-</sup>) using an ensemble of models. Collins et al. (2002) also presented GWP<sub>100</sub> estimates of 1.8 to 5.5 (−50 to +100 % uncertainty) due to CH<sub>4</sub> and O<sub>3</sub>, but for individual anthropogenic NMVOCs globally.

Using global models of chemical transport and radiative transfer, we simulate the air quality and net RF impacts, via changes in O<sub>3</sub>, CH<sub>4</sub>, and SO<sub>4</sub><sup>2-</sup>, of halving all anthropogenic NMVOC emissions together, globally and from 10 regions, as was done for CO emissions by Fry et al. (2013). We evaluate the sensitivity of air quality and RF to NMVOC emission location, and the corresponding NMVOC GWPs, which may support

Title Page

Abstract

Introduction

Conclusions

References

Tables

Figures

◀

▶

Back

Close

Full Screen / Esc

Printer-friendly Version

Interactive Discussion



the inclusion of NMVOCs in multi-gas emission trading schemes for climate. We do not consider reductions in co-emitted species that would be affected by measures to reduce NMVOCs. Future studies could evaluate the impacts of measures on multiple species, or combine the results presented here with those for co-emitted species to determine the net effect of emission control measures (Shindell et al., 2012).

## 2 Methods

### 2.1 Global chemical transport model

We evaluate the impacts on surface air quality and tropospheric composition of halving anthropogenic NMVOC emissions globally and from 10 regions (North America (NA),

10 South America (SA), Europe (EU), Former Soviet Union (FSU), Southern Africa (AF), India (IN), East Asia (EA), Southeast Asia (SE), Australia and New Zealand (AU), and Middle East and Northern Africa (ME) (Fig. S1) (Fry et al., 2013). We use the global chemical transport model (CTM), Model for OZone And Related chemical Tracers version 4 (MOZART-4) (Emmons et al., 2010).

15 The base and CH<sub>4</sub> control (where global CH<sub>4</sub> was reduced by 20 %) simulations are documented in a previous study in which the base simulation was shown to generally agree with surface and tropospheric observations (Fry et al., 2013). Here we simulate new perturbation experiments that reduce regional and global anthropogenic NMVOC

emissions by 50 % for 1 July 2004 through 31 December 2005 using MOZART-4 at a horizontal resolution of 1.9° latitude × 2.5° longitude with 56 vertical levels. We use the Coupled Model Intercomparison Project phase 5 (CMIP5) Representative Concentration Pathway 8.5 (RCP8.5) emissions inventory for the year 2005 (Riahi et al., 2007,

20 2011) and global meteorology from the Goddard Earth Observing System Model, version 5 (GEOS-5) (2004 to 2006) (Rienecker et al., 2008). Anthropogenic emissions include all anthropogenic sectors except biomass burning emissions (Fig. S2), which are excluded since actions to address biomass burning differ from the other anthro-

## Air quality and RF impacts of VOC emissions

M. M. Fry et al.

pogenic sectors, and would likely reduce a suite of emissions simultaneously (Naik et al., 2007).

RCP8.5 NMVOC species are re-specified to MOZART-4 NMVOC categories, and monthly temporal variation is added to all anthropogenic species and source categories, except for shipping, aircraft, and biomass burning, which already have monthly temporal variation (Fig. S2, Table S1). The Model of Emissions of Gases and Aerosols from Nature (MEGAN) (Guenther et al., 2006) within MOZART-4 calculates the biogenic emissions of isoprene and monoterpenes ( $C_{10}H_{16}$ ) (global annual totals of 738 Tg C yr<sup>-1</sup> and 107 Tg C yr<sup>-1</sup>, respectively), while all other natural emissions are from Emmons et al. (2010) (Table S2). The global annual lightning NO<sub>x</sub> and soil NO<sub>x</sub> emissions are also calculated by MOZART-4 as 2.4 Tg N yr<sup>-1</sup> and 8.0 Tg N yr<sup>-1</sup> (Fry et al., 2013).

Because the perturbation simulations are only 1.5 yr in length, we account for the influence of NMVOC emissions on  $\text{CH}_4$  (via OH), and thus long-term changes in  $\text{O}_3$  on the decadal timescale of the  $\text{CH}_4$  perturbation lifetime, using methods from previous studies (Prather et al., 2001; West et al., 2007; Fiore et al., 2009; and Fry et al., 2012). Global  $\text{CH}_4$  is set to a uniform mixing ratio of 1783 parts per billion by volume (ppbv) (WMO, 2006) in the base and perturbation simulations. The  $\text{CH}_4$  control simulation reduced global  $\text{CH}_4$  to 1426.4 ppbv. The results from the base and  $\text{CH}_4$  control simulations were used by Fry et al. (2013) to estimate  $\text{CH}_4$  lifetime against loss by tropospheric OH ( $\tau_{\text{OH}}$ , 11.24 yr), total  $\text{CH}_4$  lifetime based on  $\tau_{\text{OH}}$  and  $\text{CH}_4$  loss to soils and the stratosphere ( $\tau_{\text{total}}$ , 9.66 yr), and methane's feedback factor ( $F$ , 1.29) by the methods of Prather et al. (2001) and Stevenson et al. (2013). We use these parameters to estimate the steady-state tropospheric  $\text{CH}_4$  change for each of the NMVOC perturbations. Long-term  $\text{O}_3$  responses are then calculated offline by scaling  $\text{O}_3$  changes from the  $\text{CH}_4$  control simulation by the ratio of the global  $\text{CH}_4$  change from each perturbation to that of the  $\text{CH}_4$  control. We add long-term  $\text{O}_3$  changes to direct short-term  $\text{O}_3$  changes to estimate the net change at steady state (West et al., 2007, 2009b; Fiore et al., 2009; Fry et al., 2012).

Title Page	
Abstract	Introduction
Inclusions	References
Tables	Figures
◀	▶
◀	▶
Back	Close
Full Screen / Esc	
Printer-friendly Version	
Interactive Discussion	



Since MOZART-4 does not have complete stratospheric chemistry (Emmons et al., 2010), we merge each simulation's steady-state (short-term + long-term) tropospheric O<sub>3</sub> distributions (in three dimensions) with the monthly mean stratospheric O<sub>3</sub> concentrations from the AC&C/SPARC (Stratospheric Processes And their Role in Climate) O<sub>3</sub> database prepared for CMIP5 (available: <http://pcmdi-cmip.llnl.gov/cmip5/forcing.html>) (Cionni et al., 2011). By omitting lower stratospheric O<sub>3</sub> changes between each perturbation and the base simulation, our RF estimates likely underestimate the full effect of NMVOC emissions (Søvde et al., 2011).

MOZART-4 accounts for the tropospheric aerosols SO<sub>4</sub><sup>2-</sup>, black carbon (BC), primary and secondary organics, NO<sub>3</sub><sup>-</sup>, dust, and sea salt aerosols (Lamarque et al., 2005). Here we focus on changes in SO<sub>4</sub><sup>2-</sup>, NO<sub>3</sub><sup>-</sup>, and SOA, as these species are most directly influenced by anthropogenic NMVOCs, where NMVOCs are precursors to SOA, and changes in oxidants affect all three aerosol species (Barth et al., 2000; Metzger et al., 2002; and Chung and Seinfeld, 2002).

## 2.2 Radiative transfer model

We use the NOAA Geophysical Fluid Dynamics Laboratory (GFDL) standalone radiative transfer model (RTM) to perform stratospheric-adjusted net RF calculations (Schwarzkopf and Ramaswamy, 1999; GFDL GAMDT, 2004; and Naik et al., 2005, 2007) as in Fry et al. (2012), with the same updates to long-lived greenhouse gases (Meinshausen et al., 2011) and solar forcing from Fry et al. (2013). Net RF is calculated as the difference between the perturbed and base cases' simulated monthly mean net radiation fluxes (net shortwave minus net longwave), in each grid cell and month, at the tropopause after stratospheric temperatures have readjusted to radiative equilibrium (Naik et al., 2007; Saikawa et al., 2009; and Fry et al., 2012). We quantify the net RF from changes in tropospheric steady-state O<sub>3</sub>, CH<sub>4</sub>, and SO<sub>4</sub><sup>2-</sup> (direct effect only), as modeled by the MOZART-4 simulations. Meteorological fields from GFDL's atmosphere model (AM2) and land model (LM2), sampled one day per month at midmonth

13, 21125–21157, 2013

Title Page

Abstract

Introduction

Conclusions

References

Tables

Figures

◀

▶

◀

▶

Back

Close

Full Screen / Esc

Printer-friendly Version

Interactive Discussion



[Title Page](#)[Abstract](#)[Introduction](#)[Conclusions](#)[References](#)[Tables](#)[Figures](#)[|◀](#)[▶|](#)[Back](#)[Close](#)[Full Screen / Esc](#)[Printer-friendly Version](#)[Interactive Discussion](#)

for the year 2005, are also used as input to the RTM simulations, representing monthly mean conditions (Naik et al., 2005).

The RTM currently does not calculate the RF of SOA and  $\text{NO}_3^-$  aerosols. We also do not account for the RF of changes in stratospheric  $\text{O}_3$ , water vapor, the carbon cycle (via  $\text{O}_3$  and nitrogen deposition, affecting plants), and  $\text{CO}_2$  (via NMVOC oxidation, which has a minor influence on the net RF of NMVOCs) (Shindell et al., 2009). We do not estimate  $\text{CO}_2$  forcing here, because this carbon is likely accounted for in  $\text{CO}_2$  inventories (Daniel and Solomon, 1998). Our RTM simulations also exclude the indirect effects of aerosols on clouds and the internal mixing of aerosols, where aerosol indirect effects are highly uncertain and may account for considerable RF beyond aerosol direct effects (Forster et al., 2007; and Shindell et al., 2013).

### 3 Tropospheric composition and surface air quality

#### 3.1 Methane and ozone

Global annual average changes in steady-state tropospheric  $\text{CH}_4$  abundance, calculated from the tropospheric  $\text{CH}_4$  loss flux diagnosed from the model (West et al., 2007; Fiore et al., 2009; and Fry et al., 2013), are largest for ME ( $-7.37 \text{ ppbv}$ ) and SA ( $-5.41 \text{ ppbv}$ ) reductions among the 10 regions (Table 1). Normalized global  $\text{CH}_4$  changes range from 0.40 to  $1.61 \text{ ppbv} \text{ CH}_4 (\text{Tg Cyr}^{-1})^{-1}$  among the 10 regions, and are most sensitive to reductions from AU, SA, SE, and AF. These are regions of low  $\text{NO}_x$ , as discussed below, where reducing NMVOCs lessens OH depletion creating greater global  $\text{CH}_4$  changes per unit emission.  $\text{CH}_4$  decreases are least sensitive to NMVOC reductions from high- $\text{NO}_x$  regions (EA, EU, FSU). Naik et al. (2005) also found greater global  $\text{CH}_4$  sensitivities for  $\text{NO}_x$  emissions from low- $\text{NO}_x$  regions (SE, SA, and AU), and lower sensitivities for high- $\text{NO}_x$  regions (EU, FSU).

Global short-term and steady-state surface  $\text{O}_3$  changes for the 10 regional reductions are nearly proportional to NMVOC emissions changes ( $R^2 = 0.69$  and  $0.81$ )

## Air quality and RF impacts of VOC emissions

M. M. Fry et al.

Title Page

Abstract

Introduction

Conclusions

References

Tables

Figures

◀

▶

Back

Close

Full Screen / Esc

Printer-friendly Version

Interactive Discussion



(Fig. S3), but not as strongly correlated as for regional CO reductions (Fry et al., 2013). NMVOC emissions produce long-term O<sub>3</sub> decreases that augment short-term decreases by 13 % for the global reduction, and by 5–18 % for the regional reductions (Fig. 1, Table 2), similar to Fiore et al. (2009) and West et al. (2007). SA, AF, and SE reductions provide more substantial long-term global surface O<sub>3</sub> changes, which account for ~ 34 to 89 % of steady-state O<sub>3</sub> decreases.

Several of the regional reductions (SA, AF, SE, and AU) in the tropics and Southern Hemisphere (SH) produce regional to intercontinental tropospheric O<sub>3</sub> column increases (Fig. 2), as the sensitivity of O<sub>3</sub> to NMVOC emissions varies by world region. All of the regional reductions slow the formation of peroxyacetyl nitrate (PAN), causing PAN to decrease regionally to hemispherically and NO<sub>x</sub> to increase regionally (Figs. S5, S6, and S7). For SA, AF, SE, and AU, these NO<sub>x</sub> increases cause O<sub>3</sub> column increases near or downwind of the region. For the other regions, decreases in NMVOCs decrease O<sub>3</sub>, outweighing the influence of NO<sub>x</sub> increases via slowing PAN production. Whether NMVOC reductions cause O<sub>3</sub> to increase or decrease depends on the regional chemical state. Here O<sub>3</sub>-NO<sub>x</sub>-VOC sensitivity is analyzed using the photochemical indicator ratios:  $P(H_2O_2)/P(HNO_3)$ , where  $P()$  refers to production rate, (H<sub>2</sub>O<sub>2</sub>)/(HNO<sub>3</sub>), and (H<sub>2</sub>O<sub>2</sub>)/(NO<sub>2</sub>) (Sillman et al., 1997; and Liu et al., 2010). The modeled indicator ratios show that NO<sub>x</sub>-sensitive conditions prevail in the tropics and southern midlatitudes, supporting the finding of tropospheric O<sub>3</sub> increases from SA, AF, SE, and AU reductions (Figs. S8, S9, and S10). The northern mid- to high latitudes more frequently exhibit VOC-sensitivity (weaker NO<sub>x</sub>-sensitivity), particularly from November to March, resulting in O<sub>3</sub> decreases.

The global distributions of steady-state surface and tropospheric O<sub>3</sub> show the greatest decreases within each reduction region, and smaller decreases intercontinentally (Figs. 2 and S4, and Table S3). Although the largest changes in surface O<sub>3</sub> occur within the hemisphere of reduction, given that inter-hemispheric transport takes ~ 1 yr (Jacob, 1999), more widespread decreases reflect global long-term O<sub>3</sub> decreases (via CH<sub>4</sub> decreases). NMVOC reductions in one region can also influence surface O<sub>3</sub> con-

centrations in other regions importantly (Tables S3 and S4). In fact, the EA, ME, and EU NMVOC reductions have an impact on US surface O<sub>3</sub> that is 43 %, 34 %, and 34 %, respectively, of that from the NA reduction. Two of the low-NO<sub>x</sub> regions (SA and SE) experience greater decreases in surface O<sub>3</sub> from foreign regions' NMVOCs than domestic NMVOCs.

The global annual average steady-state tropospheric O<sub>3</sub> burden decreases by 0.073 Tg O<sub>3</sub> (TgCyr<sup>-1</sup>)<sup>-1</sup> for the global reduction and by -0.008 to 0.101 TgO<sub>3</sub>(TgCyr<sup>-1</sup>)<sup>-1</sup> for the 10 regions (Table 1). Changes in O<sub>3</sub> production ( $\Delta P$ ) and export ( $\Delta X$ ) are also calculated to determine the importance of long-range transport of O<sub>3</sub> and its precursors. For most regions, changes in O<sub>3</sub> production outside of each reduction region exceed changes in O<sub>3</sub> export from each region, suggesting that the influence of NMVOC emissions on the downwind production of O<sub>3</sub> has a greater impact on long-range O<sub>3</sub> than the formation and export of O<sub>3</sub> from each region (Table 1). In contrast, for the SA, AF, and SE reductions,  $\Delta X$  is positive due to regional O<sub>3</sub> increases. O<sub>3</sub> production outside the reduction region decreases for AF and SE, yet increases for SA, as SA causes widespread increases in tropospheric O<sub>3</sub> (Fig. 2). For AU, regional tropospheric O<sub>3</sub> export decreases, while tropospheric O<sub>3</sub> production increases outside AU (Table 1, Fig. 2).

### 3.2 Aerosols

NMVOC reductions affect the oxidation of SO<sub>2</sub>, NO<sub>x</sub>, monoterpenes, and toluene, influencing tropospheric SO<sub>4</sub><sup>2-</sup>, NO<sub>3</sub><sup>-</sup>, and SOA concentrations. Reductions from regions near the equator and in drier areas (SA, AF, IN, SE, and ME) produce widespread SO<sub>4</sub><sup>2-</sup> increases (Fig. 3), related to increased gas-phase SO<sub>2</sub> oxidation by OH. In fact, most of the regional reductions, except EA and AU, produce localized increases in SO<sub>4</sub><sup>2-</sup> over drier areas (e.g., Middle East and India). Tropospheric O<sub>3</sub> increases from the SA, AF, and SE reductions also contribute to SO<sub>4</sub><sup>2-</sup> increases via enhanced aqueous-phase SO<sub>2</sub> oxidation by O<sub>3</sub>, where aqueous-phase SO<sub>2</sub> oxidation is more efficient than

Air quality and RF impacts of VOC emissions

M. M. Fry et al.

Title Page

Abstract

Introduction

Conclusions

References

Tables

Figures

◀

▶

◀

▶

Back

Close

Full Screen / Esc

Printer-friendly Version

Interactive Discussion



Title Page

Abstract

Introduction

Conclusions

References

Tables

Figures

◀

▶

Back

Close

Full Screen / Esc

Printer-friendly Version

Interactive Discussion



gas-phase oxidation (Unger et al., 2006). Regional reductions in the northern midlatitudes (NA, EU, FSU, and EA) result in widespread decreases in  $\text{SO}_4^{2-}$ , due to the prevalence of clouds and decreased aqueous-phase oxidation (in clouds) of  $\text{SO}_2$  by  $\text{O}_3$  and  $\text{H}_2\text{O}_2$  (Figs. 3, S11, and S12).  $\text{NO}_3^-$  changes include both regional increases

5 and decreases. As with  $\text{SO}_4^{2-}$ ,  $\text{NO}_3^-$  increases are expected due to OH increases that are global in scale, yet largest over the source region (Figs. S13 and S14). SOA decreases globally, influenced not only by oxidant changes, but also by NMVOCs directly, as NMVOCs are precursors to SOA. The largest SOA decreases occur over the reduction region (Fig. S15). While MOZART-4 accounts for SOA formation through the 10 oxidation of monoterpenes and toluene, more research is needed to more fully model SOA. Current models greatly simplify the physical and chemical processes contributing to SOA burden, and underpredict SOA formation compared to observations (Carlton et al., 2009).

Global annual average  $\text{SO}_4^{2-}$  burden decreases for most regional reductions, yet increases for SA, AF, and ME (Table 3). For all 10 regional reductions, global  $\text{NO}_3^-$  burden increases and global SOA burden decreases. The sums of global burden changes for all 10 regional reductions, for  $\text{SO}_4^{2-}$ ,  $\text{NO}_3^-$ , and SOA, are 95 to 99 % of the burden changes for the global NMVOC reduction, suggesting some dependence on regional conditions and chemistry.

## 20 4 Radiative forcing and global warming potential

The global annual average net RF is estimated as  $-9.73 \text{ mW m}^{-2}$  for the global 50 % NMVOC reduction or  $0.21 \text{ mW m}^{-2} (\text{Tg Cyr}^{-1})^{-1}$  (Table 4). To compare with other estimates of anthropogenic forcing, we double this net RF and scale for biomass burning emissions (29.9 % of global anthropogenic NMVOC emissions), which were excluded in the 50 % reductions, yielding a global net RF of  $-0.0277 \text{ W m}^{-2}$ . This approach assumes that biomass burning emissions have the same locations and mixture of NMVOCs as anthropogenic emissions. This RF is  $\sim 49$  % of the ACCMIP

## Air quality and RF impacts of VOC emissions

M. M. Fry et al.

Title Page

Abstract

Introduction

Conclusions

References

Tables

Figures

◀

▶

Back

Close

Full Screen / Esc

Printer-friendly Version

Interactive Discussion



## Air quality and RF impacts of VOC emissions

M. M. Fry et al.

[Title Page](#)

[Abstract](#)

[Introduction](#)

[Conclusions](#)

[References](#)

[Tables](#)

[Figures](#)

[|◀](#)

[▶|](#)

[◀](#)

[▶|](#)

[Back](#)

[Close](#)

[Full Screen / Esc](#)

[Printer-friendly Version](#)

[Interactive Discussion](#)



slight regional cooling and warming effects. Globally,  $\text{NO}_3^-$  and SOA would contribute small negative and positive RFs, respectively, to global net RF.

Using the methods of Collins et al. (2013) and Fry et al. (2012, 2013), we calculate GWPs for each reduction as the RF integrated to 20 and 100 yr, normalized by the emissions change, and divided by the equivalent for  $\text{CO}_2$  (Table 4). These GWPs represent short-term contributions from  $\text{SO}_4^{2-}$  and  $\text{O}_3$  (assumed constant over one year and zero thereafter), and long-term contributions of  $\text{CH}_4$  and  $\text{O}_3$  (responding and decaying with the  $\text{CH}_4$  perturbation lifetime of 12.48 yr) (Fry et al., 2013). The long-term  $\text{O}_3$  RF component is calculated by scaling the  $\text{O}_3$  RF from the  $\text{CH}_4$  control simulation by the ratio of the long-term  $\text{O}_3$  burden change from each perturbation to that of the  $\text{CH}_4$  control. Short-term  $\text{O}_3$  RF is the difference between steady-state  $\text{O}_3$  RF (simulated by the RTM) and long-term  $\text{O}_3$  RF.

$\text{GWP}_{20}$  and  $\text{GWP}_{100}$  are estimated as 5.83 and 2.36, respectively, for the global reduction, and  $-1.13$  to 18.9 and 0.079 to 6.05 among the 10 regions, suggesting strong dependence on emission location, consistent with the normalized net RFs (Fig. 5).  $\text{GWP}_{20}$  and  $\text{GWP}_{100}$  are greatest for ME, which also had the largest net RF sensitivity, and smallest for EA, because of the nearly equivalent (opposing) short- and long-term effects. SA, SE, and AU reductions yield the largest (negative) short-term components for  $\text{GWP}_{20}$  and  $\text{GWP}_{100}$  due to the combined effect of  $\text{SO}_4^{2-}$  and tropospheric  $\text{O}_3$  increases, which act in the opposite direction to the long-term component. Uncertainty in NMVOC GWPs is based on the spread across an ensemble of global CTMs from Fry et al. (2012) ( $\pm 1$  standard deviation,  $\text{GWP}_{20}: \pm 6.0$  and  $\text{GWP}_{100}: \pm 2.1$ ), but do not account for the full uncertainty, as additional forcings could change net RF and GWP estimates.

Our GWPs (and RFs) do not include the forcing from  $\text{CO}_2$  as NMVOCs oxidize, since carbon emissions are often accounted for in  $\text{CO}_2$  inventories (Fuglestvedt et al., 1996; Daniel and Solomon, 1998; and Collins et al., 2002). Including  $\text{CO}_2$  forcing, however, may provide a more complete accounting of the effects of NMVOCs, increasing each  $\text{GWP}_{20}$  and  $\text{GWP}_{100}$  estimate by 3.67 ( $44 \text{ g CO}_2 \text{ mol}^{-1}$  ( $56.6 \text{ g C mol}^{-1}$ ) $^{-1}$  \* 4.7 C per

NMVOC molecule), based on the global annual average molecular weight and number of carbons per molecule for anthropogenic NMVOC emissions. This increases the global GWP<sub>20</sub> and GWP<sub>100</sub> by 63 % and 155 %, respectively, and makes all regional GWP<sub>20</sub> and GWP<sub>100</sub> estimates positive.

The GWP<sub>20</sub> and GWP<sub>100</sub> estimates for NA, EU, and IN (South Asia) reductions are approximately 32 to 41 %, 61 to 69 %, and 50 to 52 % lower than the multimodel mean estimates of Fry et al. (2012) (Table S10). EA GWP<sub>20</sub> and GWP<sub>100</sub> estimates, being near zero, also greatly contrast with Fry et al. (2012). Here total NMVOC/NO<sub>x</sub> emissions ratios are 57 % greater globally and in NA than the multimodel mean ratios, partly due to greater biogenic NMVOC emission sources (calculated online in MOZART-4). In EU, EA, and IN, the total NMVOC/NO<sub>x</sub> emissions are closer to the multimodel mean ratios: 4 % and 9 % (EU and EA, respectively) less and 8 % (IN) greater than those of the multimodel mean (Table S11). Global O<sub>3</sub> burden responses (in Tg O<sub>3</sub> (TgCyr<sup>-1</sup>)<sup>-1</sup>) are 27 % to 51 % less than those in Fry et al. (2012), likely due to the greater NMVOC/NO<sub>x</sub> emission ratios in this study, which would suggest less sensitivity to NMVOC emissions, but differences in the representations of NMVOCs and oxidation chemistry among models may also contribute to these differences. Global SO<sub>4</sub><sup>2-</sup> responses (in Gg SO<sub>4</sub><sup>2-</sup> (TgCyr<sup>-1</sup>)<sup>-1</sup>) also highly vary, more commonly causing increases in SO<sub>4</sub><sup>2-</sup> compared to the decreases in Fry et al. (2012) (Table S12). Collins et al. (2002) calculated GWP<sub>100</sub> estimates for individual NMVOC species (due to CH<sub>4</sub> and O<sub>3</sub> only) ranging from 1.9 to 5.5 (-50 % to 100 % uncertainty), which are more similar to the GWP<sub>100</sub> magnitudes estimated here. While our NMVOC GWP estimates consider all anthropogenic NMVOCs together and are derived from only one CTM and RTM, they represent emissions from a greater number of regions, including the tropics and extra-tropics.

Air quality and RF  
impacts of VOC  
emissions

M. M. Fry et al.

Title Page

Abstract

Introduction

Conclusions

References

Tables

Figures

◀

▶

Back

Close

Full Screen / Esc

Printer-friendly Version

Interactive Discussion



## 5 Summary

Reducing NMVOC emissions provides regional to global benefits to air quality and climate. Halving anthropogenic NMVOCs from each region creates widespread small negative net RFs across both hemispheres from global CH<sub>4</sub> and long-term O<sub>3</sub> decreases.

- 5 RF is also negative near several source regions (e.g., IN, ME) due to regional SO<sub>4</sub><sup>2-</sup> increases and short-term O<sub>3</sub> decreases. Regional small positive RFs correspond to regional SO<sub>4</sub><sup>2-</sup> decreases (e.g., NA, EU, FSU, EA, and SE) and tropospheric O<sub>3</sub> increases (e.g., SA, AF, SE, and AU).

The present-day NMVOC RF is estimated as 0.0277 W m<sup>-2</sup>, or ~1.8% of CO<sub>2</sub> 10 RF since the preindustrial. Our RF, GWP<sub>20</sub>, and GWP<sub>100</sub> estimates for the NA, EA, EU, and IN reductions are also lower than the multimodel mean estimates of Fry et al. (2012), due to differences in O<sub>3</sub>-NO<sub>x</sub>-VOC sensitivities and SO<sub>4</sub><sup>2-</sup> responses, and in particular, because of regional O<sub>3</sub> increases and SO<sub>4</sub><sup>2-</sup> decreases for some 15 regions that oppose the long-term cooling. Considerable variability in the global net RF, GWP<sub>20</sub>, and GWP<sub>100</sub> estimates among regions suggests a strong dependence on emission location: 0.21 mW m<sup>-2</sup> (Tg C yr<sup>-1</sup>)<sup>-1</sup>, 5.83, and 2.36 for the global reduction, and 0.30 ± 0.15 mW m<sup>-2</sup> (Tg C yr<sup>-1</sup>)<sup>-1</sup>, -1.13 to 18.9, and 0.079 to 6.05 for the 10 regions. GWP<sub>20</sub> and GWP<sub>100</sub> are greatest for regions in the tropics and SH (i.e., ME, IN, and AF) and less for regions in the northern midlatitudes (i.e., EU and FSU). The lowest 20 GWP<sub>20</sub> and GWP<sub>100</sub> estimates are for EA, given the nearly equivalent (opposing) short- and long-term effects. Including additional forcings beyond CH<sub>4</sub>, O<sub>3</sub>, and SO<sub>4</sub><sup>2-</sup> would likely change RF and GWP estimates.

Variability in global annual average tropospheric CH<sub>4</sub>, O<sub>3</sub>, and SO<sub>4</sub><sup>2-</sup> responses contribute to the RF and GWP differences seen among regions: 0.81 ppbv CH<sub>4</sub> 25 (Tg C yr<sup>-1</sup>)<sup>-1</sup>, 0.073 Tg O<sub>3</sub> (Tg C yr<sup>-1</sup>)<sup>-1</sup>, and 0.33 Gg SO<sub>4</sub><sup>2-</sup> (Tg C yr<sup>-1</sup>)<sup>-1</sup> for the global reduction, and 0.40 to 1.61 ppbv CH<sub>4</sub> (Tg C yr<sup>-1</sup>)<sup>-1</sup>, -0.008 to 0.101 Tg O<sub>3</sub> (Tg C yr<sup>-1</sup>)<sup>-1</sup>, and -0.21 to 1.01 Gg SO<sub>4</sub><sup>2-</sup> (Tg C yr<sup>-1</sup>)<sup>-1</sup> among the 10 regions. Sev-

## Air quality and RF impacts of VOC emissions

M. M. Fry et al.

[Title Page](#)

[Abstract](#)

[Introduction](#)

[Conclusions](#)

[References](#)

[Tables](#)

[Figures](#)

◀

▶

◀

▶

[Back](#)

[Close](#)

[Full Screen / Esc](#)

[Printer-friendly Version](#)

[Interactive Discussion](#)



eral regions with high GWPs are low- $\text{NO}_x$  regions (AF and AU), which have stronger  $\text{CH}_4$  sensitivities to NMVOC reductions, and weak increases or decreases in  $\text{SO}_4^{2-}$ .

Anthropogenic NMVOC emissions overall contribute  $\sim 5.1\%$  (1.9 ppbv) to global annual average steady-state surface  $\text{O}_3$ , by doubling the change from the 50% global NMVOC reduction ( $-0.67$  ppbv) and scaling for biomass burning emissions. Some regional reductions contribute importantly to surface  $\text{O}_3$  in other regions, such as EA, ME, and EU, which impact US surface  $\text{O}_3$  by 43%, 34%, and 34%, respectively, of that from NA emissions. NMVOC emission reductions mostly have a greater impact on downwind  $\text{O}_3$  production than the formation and export of  $\text{O}_3$  from each source region. Long-term surface  $\text{O}_3$  changes (via  $\text{CH}_4$ ) impact air quality globally, and for most regions add 5–18% to short-term changes.

In this study, the air quality and RF impacts are derived from one CTM and RTM, which limits our ability to capture a more complete range of  $\text{CH}_4$ ,  $\text{O}_3$ , aerosols, and RF responses, as a model ensemble would. Previous studies have shown a large model spread in  $\text{CH}_4$ ,  $\text{O}_3$ , and  $\text{SO}_4^{2-}$  responses to regional NMVOC emissions (Collins et al., 2002; Fiore et al., 2009; and Fry et al., 2012). Future work could examine the emissions inventories of NMVOCs and other species, as they are fairly uncertain among models (Berntsen et al., 2005).

Other limitations include only accounting for  $\text{CH}_4$ ,  $\text{O}_3$ , and  $\text{SO}_4^{2-}$  (direct effect only) in our net RF and GWP estimates, which may affect the magnitude of our estimates and variability among regions. Forcing mechanisms not accounted for include  $\text{NO}_3^-$ , SOA, stratospheric  $\text{O}_3$ , water vapor, the carbon cycle (via  $\text{O}_3$  and nitrogen deposition), the indirect effects of aerosols, and the internal mixing of aerosols. Future research could include these additional forcings and their uncertainty. The contribution of anthropogenic NMVOCs to SOA, in particular, is fairly uncertain, and often underpredicted by models (Volkamer et al., 2006). The influence of climate feedbacks on chemistry and future changes in emissions also may alter the air quality and RF sensitivities estimated here for present-day emissions. In addition, while we focus on the sensitivity of air quality and RF to NMVOC emissions, which is useful in determining the GWP of

[Title Page](#)[Abstract](#)[Introduction](#)[Conclusions](#)[References](#)[Tables](#)[Figures](#)[|◀](#)[▶|](#)[◀](#)[▶|](#)[Back](#)[Close](#)[Full Screen / Esc](#)[Printer-friendly Version](#)[Interactive Discussion](#)

NMVOCS, emission control measures would likely affect co-emitted species. Our results can be combined with those for co-emitted pollutants to evaluate the net effect of measures affecting multiple pollutants. Full climate responses also could be evaluated, as in Shindell and Faluvegi (2009).

- These findings of high variability in GWPs among regions for NMVOCS contrast with our earlier findings for CO, with little variability in GWPs among source regions (Fry et al., 2013). While it would be possible to include CO in multi-gas emissions trading schemes using a single GWP, with little error, using a single GWP for NMVOCS would cause significant error. Instead, international climate agreements could consider including NMVOCS in multi-gas emissions trading schemes using GWPs that are specific to each region. Although NMVOCS are a small climate forcing agent, this study motivates reductions in NMVOC emissions as part of future coordinated policies addressing air quality and climate change (Rypdal et al., 2005, 2009; Jackson et al., 2009; Shindell et al., 2012; and Fry et al., 2013).

Supplementary material related to this article is available online at  
[http://www.atmos-chem-phys-discuss.net/13/21125/2013/  
acpd-13-21125-2013-supplement.pdf](http://www.atmos-chem-phys-discuss.net/13/21125/2013/acpd-13-21125-2013-supplement.pdf).

Acknowledgements. This research has been funded by the US EPA under the Science to Achieve Results (STAR) Graduate Fellowship Program (M. Fry), and by the US EPA Office of Air Quality Planning and Standards. EPA has not officially endorsed this report, and the views expressed herein may not reflect the views of EPA. We acknowledge contributions from V. Naik (UCAR/NOAA GFDL) to the methodology and development of the manuscript. We also thank L. Emmons (UCAR) for observation comparison tools, L. Emmons and S. Walters (UCAR) for MOZART-4 guidance, and W. J. Collins (University of Reading) for GWP calculation methodology.

Air quality and RF  
impacts of VOC  
emissions

M. M. Fry et al.

Title Page

Abstract

Introduction

Conclusions

References

Tables

Figures

◀

▶

◀

▶

Back

Close

Full Screen / Esc

Printer-friendly Version

Interactive Discussion



## References

## Air quality and RF impacts of VOC emissions

M. M. Fry et al.

[Title Page](#)

[Abstract](#)

[Introduction](#)

[Conclusions](#)

[References](#)

[Tables](#)

[Figures](#)

[|◀](#)

[▶|](#)

[◀](#)

[▶|](#)

[Back](#)

[Close](#)

[Full Screen / Esc](#)

[Printer-friendly Version](#)

[Interactive Discussion](#)



## Air quality and RF impacts of VOC emissions

M. M. Fry et al.

[Title Page](#)

[Abstract](#)

[Introduction](#)

[Conclusions](#)

[References](#)

[Tables](#)

[Figures](#)

[◀](#)

[▶](#)

[◀](#)

[▶](#)

[Back](#)

[Close](#)

[Full Screen / Esc](#)

[Printer-friendly Version](#)

[Interactive Discussion](#)



cursor emissions from four world regions on tropospheric composition and radiative climate forcing, *J. Geophys. Res.*, 117, D07306, doi:10.1029/2011JD017134, 2012.

Fry, M. M., Schwarzkopf, M. D., Adelman, Z., Naik, V., Collins, W. J., and West, J. J.: Net radiative forcing and air quality responses to regional CO emission reductions, *Atmos. Chem. Phys.*, 13, 5381–5399, doi:10.5194/acp-13-5381-2013, 2013.

Fuglestvedt, J. S., Isaksen, I. S. A., and Wang, W.-C.: Estimates of indirect global warming potentials for CH<sub>4</sub>, CO, and NO<sub>x</sub>, *Climatic Change*, 34, 405–437, 1996.

GFDL Global Atmospheric Model Development Team (GAMDT): The new GFDL global atmosphere and land model AM2-LM2: evaluation with prescribed SST simulations, *J. Climate*, 17, 4641–4673, 2004.

Guenther, A., Karl, T., Harley, P., Wiedinmyer, C., Palmer, P. I., and Geron, C.: Estimates of global terrestrial isoprene emissions using MEGAN (Model of Emissions of Gases and Aerosols from Nature), *Atmos. Chem. Phys.*, 6, 3181–3210, doi:10.5194/acp-6-3181-2006, 2006.

Hoyle, C. R., Myhre, G., Berntsen, T. K., and Isaksen, I. S. A.: Anthropogenic influence on SOA and the resulting radiative forcing, *Atmos. Chem. Phys.*, 9, 2715–2728, doi:10.5194/acp-9-2715-2009, 2009.

Ito, A., Sillman, S., and Penner, J. E.: Effects of additional nonmethane volatile organic compounds, organic nitrates, and direct emissions of oxygenated organic species on global tropospheric chemistry, *J. Geophys. Res.*, 112, D06309, doi:10.1029/2005JD006556, 2007.

Jackson, S. C.: Parallel pursuit of near-term and long-term climate mitigation, *Science*, 326, 5952, 526–527, doi:10.1126/science.1177042, 2009.

Jacob, D. J.: Introduction to Atmospheric Chemistry, Princeton University Press, Princeton, NJ, USA, 52–53, 1999.

Lamarque, J.-F., Kiehl, J. T., Hess, P. G., Collins, W. D., Emmons, L. K., Ginoux, P., Luo, C., and Tie, X. X.: Response of a coupled chemistry-climate model to changes in aerosol emissions: global impact on the hydrological cycle and the tropospheric burdens of OH, ozone, and NO<sub>x</sub>, *Geophys. Res. Lett.*, 32, L16809, doi:10.1029/2005GL023419, 2005.

Leibensperger, E. M., Mickley, L. J., Jacob, D. J., and Barrett, S. R. H.: Intercontinental influence of NO<sub>x</sub> and CO emissions on particulate matter air quality, *Atmos. Environ.*, 45, 3318–3324, doi:10.1016/j.atmosenv.2011.02.023, 2011.

Liu, X.-H., Zhang, Y., Xing, J., Zhang, Q., Wang, K., Streets, D. G., Jang, C., Wang, W.-X., and Hao, J.-M.: Understanding of regional air pollution over China using CMAQ, part II.

[Title Page](#)

[Abstract](#)

[Introduction](#)

[Conclusions](#)

[References](#)

[Tables](#)

[Figures](#)

[◀](#)

[▶](#)

[◀](#)

[▶](#)

[Back](#)

[Close](#)

[Full Screen / Esc](#)

[Printer-friendly Version](#)

[Interactive Discussion](#)



Process analysis and sensitivity of ozone and particulate matter to precursor emissions, *Atmos. Environ.*, 44, 3719–3727, 2010.

Meinshausen, M., Smith, S. J., Calvin, K. V., Daniel, J. S., Kainuma, M. L. T., Lamarque, J.-F., Matsumoto, K., Montzka, S. A., Raper, S. C. B., Riahi, K., Thomson, A. M., Velders, G. J. M., and van Vuuren, D.: The RCP greenhouse gas concentrations and their extension from 1765 to 2300, *Climatic Change* (Special Issue), 109, 213–241, doi:10.1007/s10584-011-0156-z, 2011.

Metzger, S., Dentener, F., Pandis, S., and Lelieveld, J.: Gas/aerosol partitioning: 1. A computationally efficient model, *J. Geophys. Res.*, 107, 4312, doi:10.1029/2001JD001102, 2002.

Naik, V., Mauzerall, D., Horowitz, L., Schwarzkopf, M. D., Ramaswamy, V., and Oppenheimer, M.: Net radiative forcing due to changes in regional emissions of tropospheric ozone precursors, *J. Geophys. Res.*, 110, D24306, doi:10.1029/2005JD005908, 2005.

Naik, V., Mauzerall, D. L., Horowitz, L. W., Schwarzkopf, M. D., Ramaswamy, V., and Oppenheimer, M.: On the sensitivity of radiative forcing from biomass burning aerosols and ozone to emission location, *Geophys. Res. Lett.*, 34, L03818, doi:10.1029/2006GL028149, 2007.

Prather, M. J.: Time scales in atmospheric chemistry: theory, GWPs for CH<sub>4</sub> and CO, and runaway growth, *Geophys. Res. Lett.*, 23, 2597–2600, doi:10.1029/96GL02371, 1996.

Prather, M., Ehhalt, D., Dentener, F., Derwent, R. G., Dlugokencky, E., Holland, E., Isaksen, I. S. A., Katima, J., Kirchhoff, V., Matson, P., Midgley, P. M., and Wang, M.: Climate Change 2001: The Scientific Basis, Atmospheric Chemistry and Greenhouse Gases, Chap. 4, Cambridge Univ. Press, New York, USA, 239–287, 2001.

Riahi, K., Gruebler, A., and Nakicenovic, N.: Scenarios of long-term socio-economic and environmental development under climate stabilization, *Technol. Forecast. Soc.*, 74, 887–935, 2007.

Riahi, K., Rao, S., Krey, V., Cho, C., Chirkov, V., Fischer, G., Kindermann, G., Nakicenovic, N., and Rafaj, P.: RCP 8.5 – a scenario of comparatively high greenhouse gas emissions, *Climatic Change*, 109, 33–57, doi:10.1007/s10584-011-0149-y, 2011.

Rienecker, M. M., Suarez, M. J., Todling, R., Bacmeister, J., Takacs, L., Liu, H.-C., Gu, W., Sienkiewicz, M., Koster, R. D., Gelaro, R., Stajner, I., and Nielsen, J. E.: The GEOS-5 Data Assimilation System – Documentation of versions 5.0.1, 5.1.0, and 5.2.0, NASA Tech. Memo., NASA/TM-2008-104606, vol. 27, 118 pp., 2008.

[Title Page](#)

[Abstract](#)

[Introduction](#)

[Conclusions](#)

[References](#)

[Tables](#)

[Figures](#)

◀

▶

[Back](#)

[Close](#)

[Full Screen / Esc](#)

[Printer-friendly Version](#)

[Interactive Discussion](#)



- Rypdal, K., Berntsen, T., Fuglestvedt, J. S., Aunan, K., Torvanger, A., Stordal, F., Pacyna, J. M., and Nygaard, L. P.: Tropospheric ozone and aerosols in climate agreements: scientific and political challenges, *Environ. Sci. Policy*, 8, 29–43, doi:10.1016/j.envsci.2004.09.003, 2005.
- Rypdal, K., Rive, N., Berntsen, T., Fagerli, H., Klimont, Z., Mideksa, T. K., and Fuglestvedt, J. S.: Climate and air quality-driven scenarios of ozone and aerosol precursor abatement, *Environ. Sci. Policy*, 12, 855–869, doi:10.1016/j.envsci.2009.08.002, 2009.
- Saikawa, E., Naik, V., Horowitz, L. W., Liu, J. F., and Mauzerall, D. L.: Present and potential future contributions of sulfate, black and organic carbon aerosols from China to global air quality, premature mortality and radiative forcing, *Atmos. Environ.*, 43, 2814–2822, doi:10.1016/j.atmosenv.2009.02.017, 2009.
- Schwarzkopf, M. D. and Ramaswamy, V.: Radiative effects of CH<sub>4</sub>, N<sub>2</sub>O, halocarbons and the foreign-broadened H<sub>2</sub>O continuum: a GCM experiment, *J. Geophys. Res.*, 104, 9467–9488, doi:10.1029/1999JD900003, 1999.
- Shindell, D. T., Faluvegi, G., Bell, N., and Schmidt, G. A.: An emissions-based view of climate forcing by methane and tropospheric ozone, *Geophys. Res. Lett.*, 32, L04803, doi:10.1029/2004GL021900, 2005.
- Shindell, D. and Faluvegi, G.: Climate response to regional radiative forcing during the twentieth century, *Nat. Geosci.*, 2, 294–300, doi:10.1038/NGEO473, 2009.
- Shindell, D. T., Faluvegi, G., Koch, D. M., Schmidt, G. A., Unger, N., and Bauer, S. E.: Improved attribution of climate forcing to emissions, *Science*, 326, 716–718, doi:10.1126/science.1174760, 2009.
- Shindell, D., Kylenstierna, J. C. I., Vignati, E., van Dingenen, R., Amann, M., Klimont, Z., Anenberg, S. C., Muller, N., Janssens-Maenhout, G., Raes, F., Schwartz, J., Faluvegi, G., Pozzoli, L., Kupiainen, K., Höglund-Isaksson, L., Emberson, L., Streets, D., Ramanathan, V., Hicks, K., Oanh, N. T. K., Milly, G., Williams, M., Demkine, V., and Fowler, D.: Simultaneously mitigating near-term climate change and improving human health and food security, *Science*, 335, 183–189, doi:10.1126/science.1210026, 2012.
- Shindell, D. T., Lamarque, J.-F., Schulz, M., Flanner, M., Jiao, C., Chin, M., Young, P. J., Lee, Y. H., Rotstayn, L., Mahowald, N., Milly, G., Faluvegi, G., Balkanski, Y., Collins, W. J., Conley, A. J., Dalsoren, S., Easter, R., Ghan, S., Horowitz, L., Liu, X., Myhre, G., Naganashima, T., Naik, V., Rumbold, S. T., Skeie, R., Sudo, K., Szopa, S., Takemura, T., Voulgarakis, A., Yoon, J.-H., and Lo, F.: Radiative forcing in the ACCMIP historical and future

[Title Page](#)

[Abstract](#)

[Introduction](#)

[Conclusions](#)

[References](#)

[Tables](#)

[Figures](#)

[◀](#)

[▶](#)

[Back](#)

[Close](#)

[Full Screen / Esc](#)

[Printer-friendly Version](#)

[Interactive Discussion](#)



Sillman, S., He, D., Cardelino, C., and Imhoff, R. E.: The use of photochemical indicators to evaluate ozone-NO<sub>x</sub>-hydrocarbon sensitivity: case studies from Atlanta, New York, and Los Angeles, *J. Air Waste Manage.*, 47, 1030–1040, 1997.

Søvde, O. A., Hoyle, C. R., Myhre, G., and Isaksen, I. S. A.: The  $\text{HNO}_3$  forming branch of the  $\text{HO}_2 + \text{NO}$  reaction: pre-industrial-to-present trends in atmospheric species and radiative forcings, *Atmos. Chem. Phys.*, 11, 8929–8943, doi:10.5194/acp-11-8929-2011, 2011.

Stevenson, D. S., Dentener, F. J., Schultz, M. G., Ellingsen, K., van Noije, T. P. C., Wild, O., Zeng, G., Amann, M., Atherton, C. S., Bell, N., Bergmann, D. J., Bey, I., Butler, T., Co-fala, J., Collins, W. J., Derwent, R. G., Doherty, R. M., Drevet, J., Eskes, H. J., Fiore, A. M., Gauss, M., Hauglustaine, D. A., Horowitz, L. W., Isaksen, I. S. A., Krol, M. C., Lamarque, J.-F., Lawrence, M. G., Montanaro, V., Müller, J.-F., Pitari, G., Prather, M. J., Pyle, J. A., Rast, S., Rodriguez, J. M., Sanderson, M. G., Savage, N. H., Shindell, D. T., Strahan, S. E., Sudo, K., and Szopa, S.: Multimodel ensemble simulations of present-day and near-future tropospheric ozone, *J. Geophys. Res.*, 111, D08301, doi:10.1029/2005JD006338, 2006.

Stevenson, D. S., Young, P. J., Naik, V., Lamarque, J.-F., Shindell, D. T., Voulgarakis, A., Skeie, R. B., Dalsoren, S. B., Myhre, G., Berntsen, T. K., Folberth, G. A., Rumbold, S. T., Collins, W. J., MacKenzie, I. A., Doherty, R. M., Zeng, G., van Noije, T. P. C., Strunk, A., Bergmann, D., Cameron-Smith, P., Plummer, D. A., Strode, S. A., Horowitz, L., Lee, Y. H., Szopa, S., Sudo, K., Nagashima, T., Josse, B., Cionni, I., Righi, M., Eyring, V., Conley, A., Bowman, K. W., Wild, O., and Archibald, A.: Tropospheric ozone changes, radiative forcing and attribution to emissions in the Atmospheric Chemistry and Climate Model Intercomparison Project (ACCMIP), *Atmos. Chem. Phys.*, 13, 3063–3085, doi:10.5194/acp-13-3063-2013, 2013.

Unger, N., Shindell, D. T., Koch, D. M., and Streets, D. G.: Cross influences of ozone and sulfate precursor emissions changes on air quality and climate, *P. Natl. Acad. Sci. USA*, 103, 4377–4380, doi:10.1073/pnas.0508769103, 2006.

Volkamer, R., Jimenez, J. L., San Martini, F., Dzepina, K., Zhang, Q., Salcedo, D., Molina, L. T., Worsnop, D. R., and Molina, M. J.: Secondary organic aerosol formation from anthropogenic air pollution: rapid and higher than expected, *Geophys. Res. Lett.*, 33, L17811, doi:10.1029/2006GL026899, 2006.

- West, J. J., Fiore, A. M., Naik, V., Horowitz, L. W., Schwarzkopf, M. D., and Mauzerall, D. L.: Ozone air quality and radiative forcing consequences of changes in ozone precursor emissions, *Geophys. Res. Lett.*, 34, L06806, doi:10.1029/2006GL029173, 2007.
- 5 West, J. J., Naik, V., Horowitz, L. W., and Fiore, A. M.: Effect of regional precursor emission controls on long-range ozone transport – Part 1: Short-term changes in ozone air quality, *Atmos. Chem. Phys.*, 9, 6077–6093, doi:10.5194/acp-9-6077-2009, 2009a.
- 10 West, J. J., Naik, V., Horowitz, L. W., and Fiore, A. M.: Effect of regional precursor emission controls on long-range ozone transport – Part 2: Steady-state changes in ozone air quality and impacts on human mortality, *Atmos. Chem. Phys.*, 9, 6095–6107, doi:10.5194/acp-9-6095-2009, 2009b.
- Wild, O., Prather, M. J., and Akimoto, H.: Indirect long-term global radiative cooling from NO<sub>x</sub> emissions, *Geophys. Res. Lett.*, 28, 1719–1722, doi:10.1029/2000GL012573, 2001.
- 15 World Meteorological Organization (WMO): WMO Greenhouse Gas Bulletin: The State of Greenhouse Gases in the Atmosphere using Global Observations through 2005, Bulletin No. 1: March 2006, 2006.

Air quality and RF  
impacts of VOC  
emissions

M. M. Fry et al.

[Title Page](#)

[Abstract](#)

[Introduction](#)

[Conclusions](#)

[References](#)

[Tables](#)

[Figures](#)

[◀](#)

[▶](#)

[Back](#)

[Close](#)

[Full Screen / Esc](#)

[Printer-friendly Version](#)

[Interactive Discussion](#)



**Table 1.** Changes in global annual average short-term and steady-state tropospheric O<sub>3</sub> burden ( $B_{O_3}$ ) and tropospheric CH<sub>4</sub> for the global and regional reductions. Changes in O<sub>3</sub> production ( $P_{O_3}$ ),  $P_{O_3}$  normalized per unit change in NMVOC emissions ( $E$ ), and  $P_{O_3}$  outside each reduction region are shown for each regional reduction. Changes in net O<sub>3</sub> export ( $X_{O_3}$ ) from each reduction region, and the fractions of  $B_{O_3}$  and  $P_{O_3}$  changes above each reduction region are also estimated.

Reduction region	$\Delta B_{O_3}$ (Tg O <sub>3</sub> ) short-term	$\Delta B_{O_3}$ (Tg O <sub>3</sub> ) steady-state	$\Delta B_{O_3}/\Delta E$ (Tg O <sub>3</sub> C <sub>yrs</sub> <sup>-1</sup> ) steady-state	$\Delta \text{CH}_4$ (ppbv)	$\Delta \text{CH}_4/\Delta E$ (Tg C <sub>yrs</sub> <sup>-1</sup> ) steady-state	$\Delta P_{O_3}/\Delta E$ (Tg yr <sup>-1</sup> )	$\Delta P_{O_3}/\Delta E$ (Tg O <sub>3</sub> C <sub>yrs</sub> <sup>-1</sup> ) steady-state	$\Delta P_{O_3}$ outside region (Tg yr <sup>-1</sup> )	$\Delta X_{O_3}$ from region (Tg yr <sup>-1</sup> )	Fraction of global $\Delta B_{O_3}$ above region	Fraction of global $\Delta P_{O_3}$ above region
NA	-0.30	-0.41	0.082	-4.05	0.80	-6.13	1.21	-3.92	-0.84	0.19	0.36
SA	0.16	0.028	-0.008	-5.41	1.60	1.95	-0.58	0.67	0.72	0.13	0.66
EU	-0.31	-0.38	0.101	-2.30	0.61	-6.15	1.64	-4.17	-1.19	0.087	0.32
FSU	-0.21	-0.25	0.101	-1.61	0.64	-3.80	1.52	-2.83	-0.48	0.21	0.25
AF	-0.081	-0.20	0.049	-4.20	1.03	-2.22	0.54	-2.34	0.41	-0.041	-0.052
IN	-0.23	-0.30	0.081	-2.40	0.65	-5.09	1.38	-3.14	-0.67	0.071	0.38
EA	-0.90	-1.02	0.099	-4.10	0.40	-18.6	1.82	-11.2	-3.79	0.10	0.40
SE	0.075	-0.066	0.016	-5.16	1.22	-0.18	0.04	-1.40	0.80	0.21	-6.75
AU	0.013	0.00	0.000	-0.54	1.61	0.19	-0.58	0.20	-0.014	0.040	-0.032
ME	-0.50	-0.69	0.091	-7.37	0.97	-9.48	1.24	-6.31	-1.79	0.10	0.33
Global	-2.44	-3.33	0.073	-36.6	0.81	-52.1	1.15	-	-	-	-

**Air quality and RF  
impacts of VOC  
emissions**

M. M. Fry et al.

**Table 2.** For the global and regional reduction simulations relative to the base, global annual average changes in short-term and steady-state surface O<sub>3</sub>.

Reduction region	ΔSurface O <sub>3</sub> short-term (pptv)	ΔSurface O <sub>3</sub> steady-state (pptv)
NA	-81.0	-89.9
SA	-1.40	-13.3
EU	-87.5	-92.6
FSU	-71.0	-74.5
AF	-18.2	-27.5
IN	-28.9	-34.2
EA	-167.1	-176.2
SE	-9.40	-20.8
AU	0.60	-0.60
ME	-100.6	-116.8
Global	-592.9	-673.5

- [Title Page](#)
- [Abstract](#) | [Introduction](#)
- [Conclusions](#) | [References](#)
- [Tables](#) | [Figures](#)
- [◀](#) | [▶](#)
- [◀](#) | [▶](#)
- [Back](#) | [Close](#)
- [Full Screen / Esc](#)
- [Printer-friendly Version](#)
- [Interactive Discussion](#)



## Air quality and RF impacts of VOC emissions

M. M. Fry et al.

**Table 3.** For the global and regional reduction simulations relative to the base, global annual average tropospheric burden changes in  $\text{SO}_4^{2-}$ ,  $\text{NO}_3^-$  (expressed as  $\text{NH}_4\text{NO}_3$ ), and SOA. The global annual average tropospheric  $\text{SO}_4^{2-}$ ,  $\text{NH}_4\text{NO}_3$ , and SOA burdens in the base simulation are 1785 Gg  $\text{SO}_4^{2-}$ , 416 Gg  $\text{NH}_4\text{NO}_3$ , and 227 Gg SOA.

Reduction region	$\Delta\text{SO}_4^{2-}$ (Gg)	$\Delta\text{NH}_4\text{NO}_3$ (Gg)	$\Delta\text{SOA}$ (Gg)
NA	-1.63	0.61	-2.91
SA	0.05	0.17	-4.57
EU	-2.26	1.47	-1.30
FSU	-1.45	0.88	-0.74
AF	0.06	0.21	-2.84
IN	-0.03	0.05	-1.66
EA	-10.3	3.21	-3.69
SE	-0.06	0.38	-5.00
AU	-0.01	0.01	-0.25
ME	1.63	0.09	-1.89
Global	-14.8	7.27	-24.9

- [Title Page](#)
- [Abstract](#) | [Introduction](#)
- [Conclusions](#) | [References](#)
- [Tables](#) | [Figures](#)
- [◀](#) | [▶](#)
- [◀](#) | [▶](#)
- [Back](#) | [Close](#)
- [Full Screen / Esc](#)
- [Printer-friendly Version](#)
- [Interactive Discussion](#)



## Air quality and RF impacts of VOC emissions

M. M. Fry et al.

**Table 4.** Annual net RF globally and by latitude band ( $\text{mW m}^{-2}$ ) and GWP<sub>20</sub> and GWP<sub>100</sub> estimates for the global and regional reduction simulations relative to the base, due to changes in tropospheric steady-state O<sub>3</sub>, CH<sub>4</sub>, and SO<sub>4</sub><sup>2-</sup> concentrations. Global annual net RF per unit change in NMVOC emissions ( $\text{mW m}^{-2} (\text{Tg Cyr}^{-1})^{-1}$ ) is also shown. The 10 regions estimate represents the sum of the net RFs from all 10 regional reductions; this estimate is not directly estimated by the RTM.

Reduction region	Global annual net RF	Global annual net RF per Tg NMVOC	Annual net RF 90–28° S	Annual net RF 28° S–28° N	Annual net RF 28–60° N	Annual net RF 60–90° N	GWP <sub>20</sub>	GWP <sub>100</sub>
NA	-1.50	0.30	-1.19	-2.13	-0.46	-2.09	9.20	3.27
SA	-1.17	0.35	-0.63	-1.20	-1.98	-1.38	8.56	3.86
EU	-0.70	0.19	-0.69	-1.46	1.05	-1.16	5.36	2.05
FSU	-0.51	0.20	-0.48	-1.05	0.58	-0.71	5.96	2.24
AF	-1.56	0.38	-1.24	-1.99	-1.79	-1.17	11.8	4.19
IN	-1.38	0.37	-0.83	-2.12	-1.54	-0.96	12.7	4.08
EA	-0.05	0.0045	-1.41	-0.24	5.98	-3.30	-1.13	0.079
SE	-1.23	0.29	-1.24	-0.79	-1.85	-1.39	7.58	3.23
AU	-0.13	0.40	0.016	-0.25	-0.21	-0.14	10.5	4.41
ME	-4.22	0.55	-2.29	-6.80	-4.56	-3.06	18.9	6.05
Global 10 regions	-9.73	0.21	-8.36	-13.8	-1.21	-14.0	5.83	2.36
	-12.5	0.28	-9.98	-18.0	-4.77	-15.3	-	-

- [Title Page](#)
- [Abstract](#) [Introduction](#)
- [Conclusions](#) [References](#)
- [Tables](#) [Figures](#)
- [◀](#) [▶](#)
- [◀](#) [▶](#)
- [Back](#) [Close](#)
- [Full Screen / Esc](#)
- [Printer-friendly Version](#)
- [Interactive Discussion](#)



# Air quality and RF impacts of VOC emissions

M. M. Fry et al.

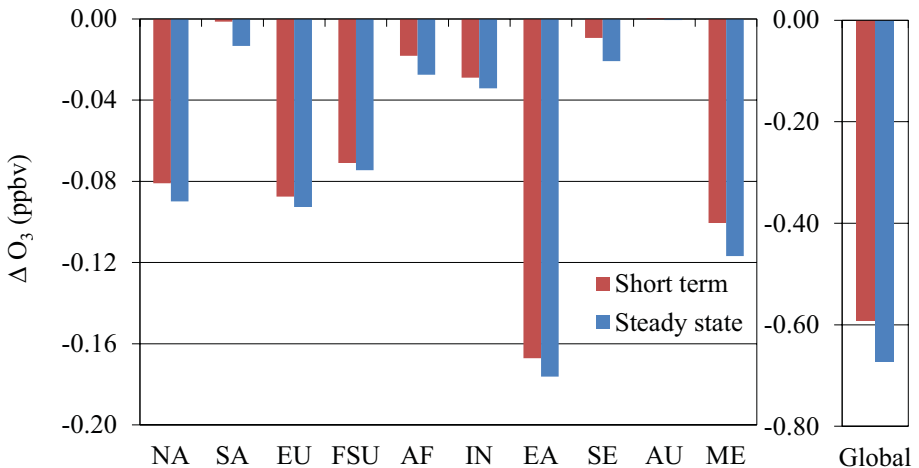


**Fig. 1.** Global annual average surface O<sub>3</sub> concentration changes (ppbv) for the regional and global reduction simulations, in the short term and at steady state.

21153

**Air quality and RF  
impacts of VOC  
emissions**

M. M. Fry et al.

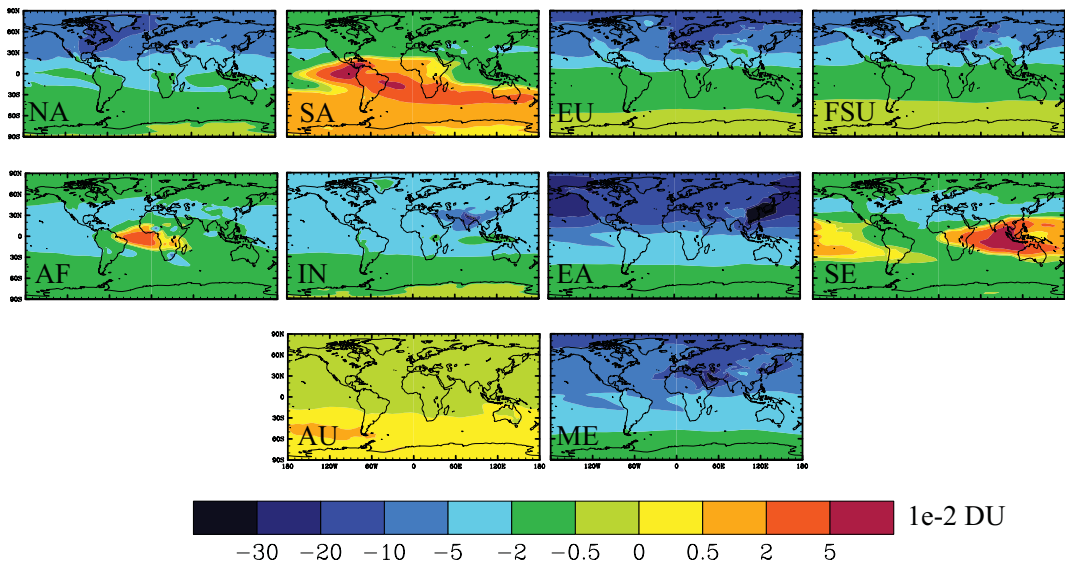


**Fig. 2.** Global distribution of annual average changes in tropospheric total column O<sub>3</sub> at steady state (1e-2 DU) for each of the regional reduction simulations relative to the base.

**Air quality and RF  
impacts of VOC  
emissions**

M. M. Fry et al.

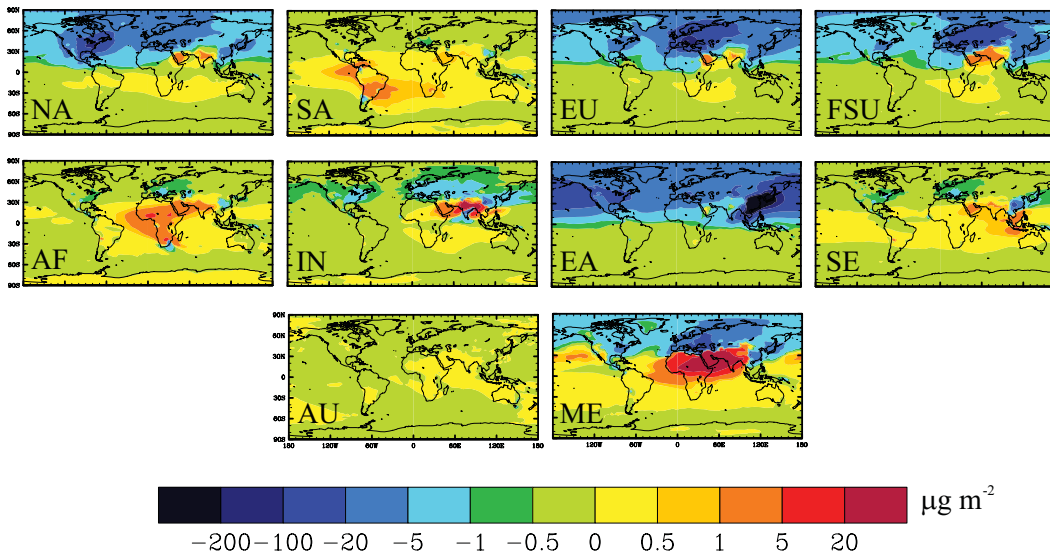


**Fig. 3.** Global distribution of annual average changes in tropospheric total column  $\text{SO}_4^{2-}$  ( $\mu\text{g m}^{-2}$ ) for each of the regional reduction simulations relative to the base.

**Air quality and RF  
impacts of VOC  
emissions**

M. M. Fry et al.

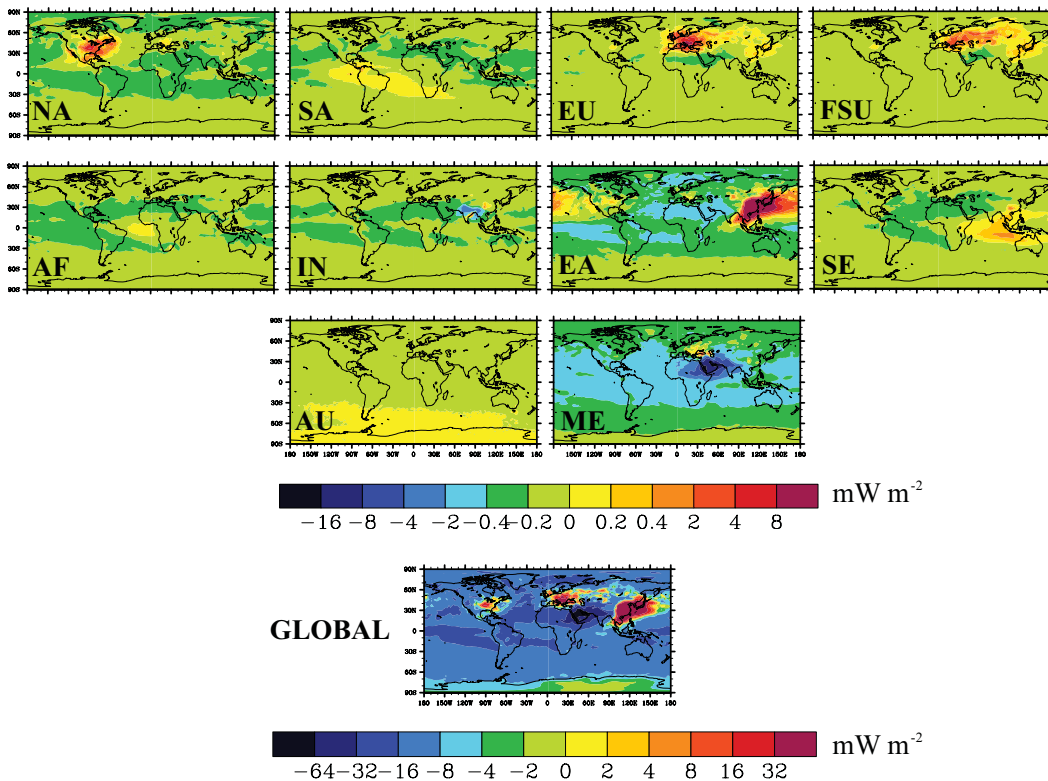


**Fig. 4.** Annual average net RF distributions ( $\text{mW m}^{-2}$ ) due to changes in tropospheric steady-state  $\text{O}_3$ ,  $\text{CH}_4$ , and  $\text{SO}_4^{2-}$  for the regional and global NMVOC reduction simulations minus the base simulation.

[Title Page](#)[Abstract](#)[Introduction](#)[Conclusions](#)[References](#)[Tables](#)[Figures](#)[|](#)[|](#)[◀](#)[▶](#)[Back](#)[Close](#)[Full Screen / Esc](#)[Printer-friendly Version](#)[Interactive Discussion](#)

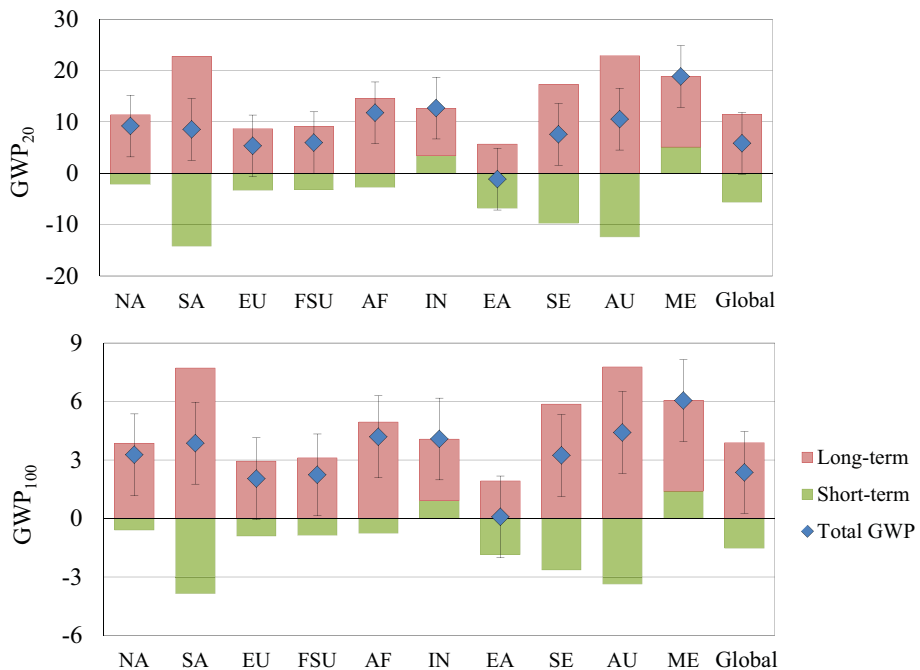


**Fig. 5.** Global warming potentials for NMVOCs at time horizons of 20 and 100 yr ( $GWP_{20}$ ,  $GWP_{100}$ ) for the regional and global reductions, with contributions from short-term ( $O_3$  and  $SO_4^{2-}$ ) and long-term ( $O_3$  and  $CH_4$ ) components, where total GWP is short-term + long-term. Uncertainty bars represent the average uncertainty found by Fry et al. (2012) based on the spread of atmospheric chemical models ( $\pm 1$  standard deviation).